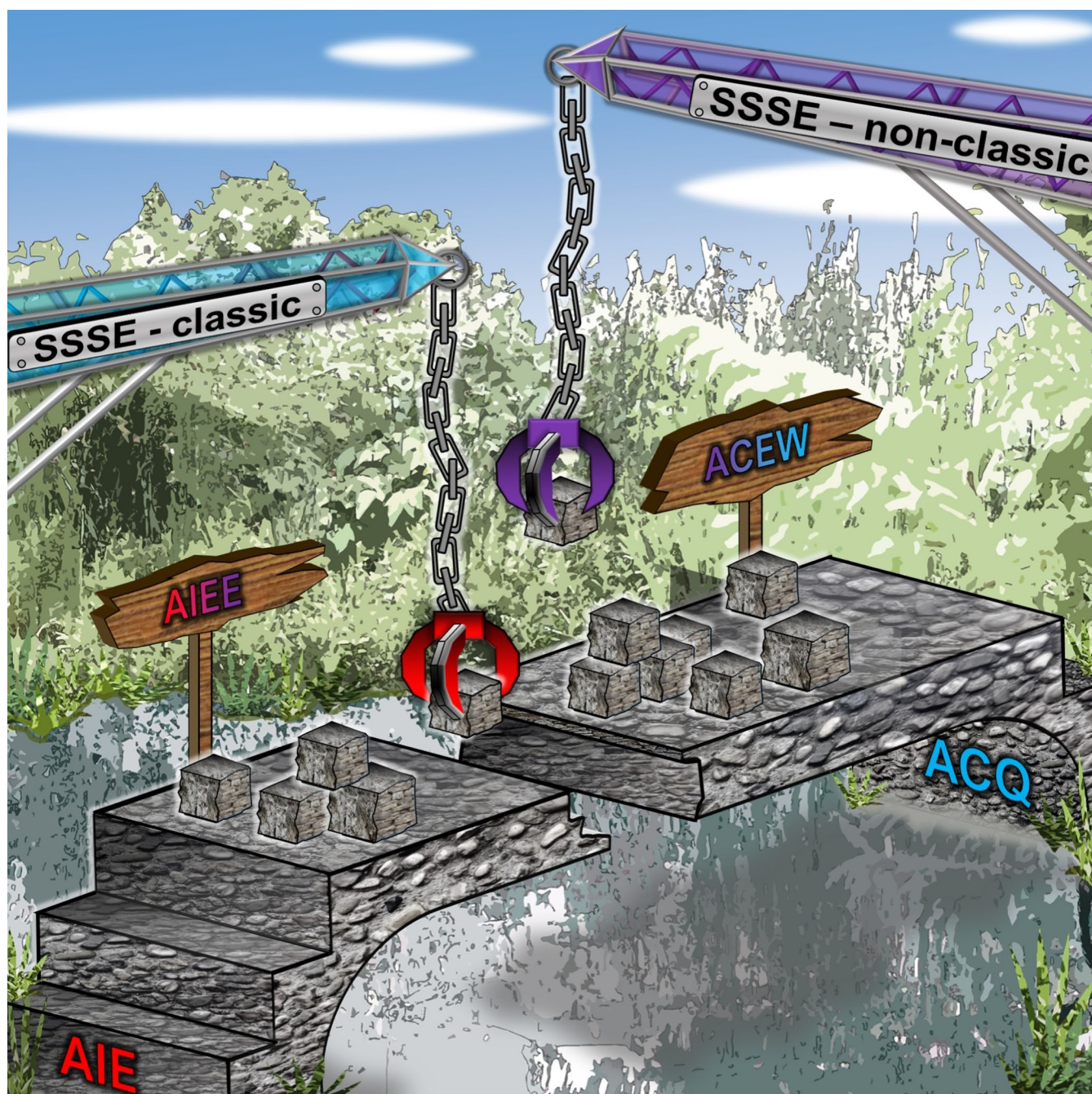


🏆 Design Concepts for Solution and Solid-State Emitters – A Modern Viewpoint on Classical and Non-Classical Approaches

Alexander Huber^{+, [a]} Justin Dubbert^{+, [a]} Tim D. Scherz^[a] and Jens Voskuhl^{*, [a]}



Abstract: For a long time, luminescence phenomena were strictly distinguished between the emission of isolated molecules in dilute solutions or close-packed structures such as in powders or aggregates. This changed with the breakthrough observation of dual-state efficient materials, which led to a rapid boost of publications examining the influence of structural features to achieve balanced emission with disregarded molecular surroundings. Some first general structural design concepts have already been proposed based

on reoccurring patterns and pivotal motifs. However, we have found another way to classify these solution and solid-state emitters (SSSEs). Hence, this minireview aims to present an overview of published structural features of SSSEs while shining light on design concepts from a more generalized perspective. Since SSSEs are believed to bridge the gap of hitherto known aggregation-sensitive compound classes, we hope to give future scientists a versatile tool in hand to efficiently design novel luminescent materials.

1. Introduction

The emissive ability of organic luminophores has been intensely investigated in the last few decades since many discoveries and technological advances were realised based on fluorescence techniques.^[1] These techniques generally display low hazard-ousness, high sensitivity, high temporal and spatial resolution, and facile feasibility.^[2] Therefore, luminescent materials have been used in various applications, for example in lasers, photovoltaic cells, spectroscopy and microscopy, and biomedical research.^[3] For each application, chemists were compelled to invent and synthesize luminescent materials with specifically tailored properties. In this regard, luminophores were designed based on the environment needed for emissive behaviour, whether in dilute organic solution, aqueous media present in cells, aggregates, thin films, crystals, or powders.

No significant efforts were made to develop an omnipotent luminophore class due to the seemingly contradictory characteristics of emissive materials in both solution and the solid-state until Tang's and co-worker's contribution in 2015 about "dual-state efficient" compounds was published.^[4] Nowadays, this phenomenon of emissive compounds in solution and the solid-state is commonly known as "dual-state emission" (DSE).^[5] Since then, the number of articles featuring keywords like "dual-state efficient", "dual-state emission" or "solution and solid-state emission" has increased gradually, according to *Web of Science*TM. However, the term "dual-state emission" is ambiguous since it also refers to emissions from different electronic states (e.g. singlet and triplet).^[6] Therefore, a numeric designation of published articles is complicated. Hence, we

prefer using the term "solution and solid-state emitters" (SSSEs) to avoid confusion.^[7,8]

In a recently appeared comprehensive review by Belmonte-Vázquez et al., almost all quantifiable SSSEs were listed and classified regarding essential structural subunits and their influence on corresponding quantum yields.^[9] Although some design concepts were proposed, formulations of general and fundamental outlines are still in the early stages, and thus distinct approaches are highly desired.

Therefore, we wish to focus in this minireview on compound classes that can emit independently of their aggregation state and provide another strategy to achieve efficient SSSEs. In this regard, we will shortly summarize classic luminescence phenomena in Section 2 and general conditions for emissive behaviour in Section 3. In Section 4 we will then concentrate on the characteristics of SSSEs regarding their molecular structure to suggest design concepts from a different viewpoint. Afterwards, these viewpoints will be discussed and presented for both classic emitters in Section 5 and non-classic emitters in Section 6. In a benchmarking Section 7, visualisation of proposed classifying conditions for SSSEs is shown before concluding and stating an outlook in Section 8.


2. Classic Luminescence Phenomena


Most organic luminophores such as perylene or fluorescein are generally aromatic because large delocalized π -electronic systems shift the wavelengths of transitioning photons towards less-energetic values. To accomplish facilitated shifting, ideally into the visible area of the electromagnetic spectrum, heteroatoms are frequently integrated into the molecular structure to induce electronic perturbation.^[10] Following excitation through low-lying π - π^* -transition, energetic dissipation in diluted solution readily takes place in the form of emission since other non-radiative deexcitation pathways occur on much slower timescales.^[11] However, it is commonly known that in the solid-state or upon aggregation, intermolecular π - π stacking interactions lead to the loss of emitting ability through non-radiative dissipation, usually referred to as "aggregation-caused quenching".^[12] Due to the ACQ effect, luminescence research in the organic field was restricted solely to dilute solutions.

Paradoxically, the contrary phenomenon of emissive compounds in the solid-state but not in solution is also long

[a] A. Huber,⁺ J. Dubbert,⁺ T. D. Scherz, Jun.-Prof. Dr. J. Voskuhl
Institute of Organic Chemistry, CENIDE and ZMB
University of Duisburg-Essen
Universitätsstrasse 7, 45117, Essen (Germany)
E-mail: jens.voskuhl@uni-due.de

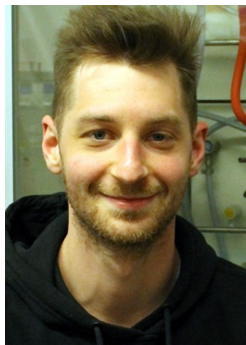
[⁺] These authors contributed equally to this manuscript.

 Selected by the Editorial Office for our Showcase of outstanding Review-type articles <http://www.chemeurj.org/showcase>.

 © 2022 The Authors. Chemistry - A European Journal published by Wiley-VCH GmbH. This is an open access article under the terms of the Creative Commons Attribution Non-Commercial License, which permits use, distribution and reproduction in any medium, provided the original work is properly cited and is not used for commercial purposes.

known.^[13] For instance, more than 100 years ago, *Gerhard C. Schmidt* observed the emissive behaviour of compounds only when embedded in solidified solutions, not when molecularly dissolved.^[14] In 1936, *Scheibe*^[15] and *Jelley*^[16] discovered a salient aggregation-induced fluorescence band of pseudoisocyanine,

Alexander Huber graduated in chemistry at the University of Duisburg-Essen. In 2019 he received his B.Sc. in the group of Prof. Dr. Jochen Niemeyer, where he worked on novel chiral [2]rotaxanes for catalysis. In 2021 he joined the group of Jun.-Prof. Dr. Jens Voskuhl for his master thesis on the topic of luminescent amphiphiles for gene delivery. He has continued his work since 2022 as a Ph.D. student, aiming for the synthesis of novel emitters for biomedical applications.



Justin Dubbert studied chemistry at the University of Duisburg-Essen, where he obtained his M.Sc. (2018) in the group of Jun.-Prof. Dr. Jens Voskuhl. At first, he worked on host-guest functionalized subphthalocyanines for usage in supramolecular chemistry. Later he continued his research in the group with the synthesis of novel luminophores with solution and solid-state emission properties for the application in bio-imaging.



Tim D. Scherz studied chemistry at the University of Duisburg-Essen. In 2019 he obtained his B.Sc. in the group of Prof. Dr.-Ing. Stephan Barcikowski with the focus on immobilization of gold-nanoparticles. After performing an analytical internship under the supervision of Jun.-Prof. Dr. Jens Voskuhl, he moved to the group of Prof. Dr. Matthias Eppe for his master thesis on the topic of surface manipulated nanoparticles. In 2022 he changed professions and is currently working at the Fire Department in Oberhausen.



Jens Voskuhl studied chemistry at the Westfälische-Wilhelms Universität Münster, where he also obtained his diploma (2008) and Ph.D. (2011) degree in the group of Bart Jan Ravoo, working on supramolecular chemistry in water. After two postdoctorates in the Netherlands (Leiden, group of Prof. Dr. Alexander Kros and Twente, group of Prof. Dr. Pascal Jonkheijm), he started his independent career at the University of Duisburg-Essen as a junior professor (2015). His research interests involve the design and application of novel luminophores for biomedicine and materials science.



now recognized as the emerging emission based on *J-aggregate formation (JAF)*.^[17] In 2001, *Tang* and co-workers described the arising emission of the propeller-shaped compound hexaphenylsilole (HPS) when aggregated.^[18] This well-cited contribution led to a research renaissance of emissive solids, terming the phenomenon "*aggregation-induced emission*" (AIE).^[38]

The quenching effect of HPS in solution was attributed to rotation processes of peripheral phenyl rings via non-radiative decays.^[19] This flexibility is hindered by the formation of aggregates at high water contents. The large torsion angles of the phenyl rings twist the structure of HPS, preventing π - π stacking, and thus, emission becomes a favourable decay process following light absorption. Although many different potential pathways were proposed, the generally accepted mechanism is believed to be this restriction of intramolecular motion (RIM), which includes both rotational (RIR) and vibrational (RIV) changes.^[20] In most cases, RIR is the more apparent reason for the appearance of AIE for example for HPS or tetraphenylethylene (TPE), albeit rigidified AIEgens, such as the annulenyldiene THBA, experience RIV. Because rotation of terminal phenyl rings is impossible, dynamic vibrations of the butterfly-like structures i. a. in-plane or out-of-plane bending, flapping, or stretching, dissipate the excitation energy in solution but get impeded upon aggregation, leading to emission of the vibrationally trapped THBA (Figure 1).^[21]

It must be stated that besides RIM, several other mechanisms for solid-state luminescence have been proposed and investigated. For instance, the previously mentioned self-assembled *J-aggregates* show a distinct emission band that has been the subject of several studies regarding their interesting intermolecular interactions.^[22] Besides viscosity increase or temperature lowering, molecular rigidification inducing emerging emission can appear as a consequence of host-guest inclusion with cyclodextrins (CDs)^[23,24] or after DNA hybridization.^[25] Because in many cases, emission is not induced solely upon aggregation but through restriction of motion, *Gierschner et al.* proposed the more proper name "*solid-state luminescence enhancement*" (SLE).^[26] Because SLE is not a commonly used abbreviation yet, we will refer to solid-state luminescent systems as AIE compounds. The arisen interest in these materials caused the exploration of wide-spread applica-

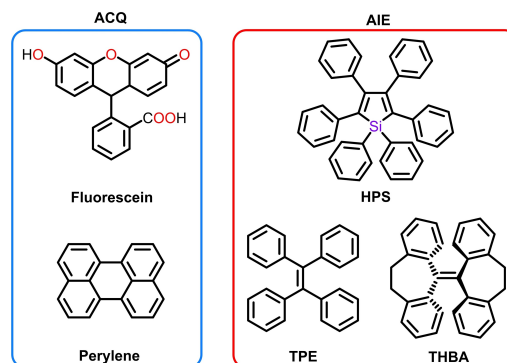


Figure 1. Chemical structures of ACQ compounds fluorescein and perylene (left) and AIE luminophores HPS, TPE, and THBA (right).

tion possibilities ranging from chemosensing^[27] over optoelectronic systems such as high-performance organic light-emitting diodes (OLEDs)^[28] to biomedical imaging,^[29,30] protein recognition,^[31] and gene therapy.^[32]

3. General Remarks and Conditions for Solution and Solid-State Emission

The previous recap highlighted the advantages and utilization importance of luminescent materials in solution and the solid-state. In this section, we will discuss the general fundamentals of high-performing emitters. The quantum yield Φ_F of a luminophore is the photophysical measurand that classifies an SSSE as efficient or inefficient because all possible radiative (r) or non-radiative (nr) deexcitation pathways are included through their respective rate constants k (Equation (1)).^[1]

$$\Phi_F = \frac{k_r}{k_r + k_{nr}} = \frac{k_r}{\sum k_i} \quad (1)$$

Some general remarks must be considered when comparing different values for Φ_F . First, measurements can be performed using the relative method by referencing literature-validated standards like quinine-sulphate or by the absolute method with an integrating sphere (Ulbricht sphere).^[33] Also, temperature has a significant effect on the observed emissive properties. However, in this minireview, we will only discuss emissive behaviour at room-temperature.

Second, although SSSE researchers endeavour molecular independence of the surrounding environment, the solvent relaxation cannot be disregarded because different polarities are known to induce distinguished stabilising forces for ground and excited states (solvatochromism).^[34] Especially for compounds with donor-acceptor (D-A) structure, intramolecular charge-transfer (ICT) is a favoured excited state process as the charge redistribution minimizes the global molecular energy compared to locally excited (LE) states.^[35] For this, reorientation mechanisms such as twisting (TICT), planarizing (PLICT), or wagging (WICT) are well-known and can facilitate decay via non-radiative channels.^[36] In this regard, the solvent acidity, basicity, or any other solvent-solute specific interaction can significantly impact phenomena like excited state proton transfers.^[37] Furthermore, solvent viscosity can be interpreted as a mediating parameter than can balance the transition of versatile movement in solution and rigidified fixation.^[38]

Third, the particular state of close-packed structures is also wide-ranging, as measurements can be conducted for emissive amorphous powders, crystalline samples, thin films, polymeric matrices, frozen solutions, or aggregates in dispersions.^[26] To be concise, we will refer to this solely by the term “solid-state”.

Considering a more fundamental view on radiative vs. non-radiative decay, non-emissive relaxation occurs through internal conversion (IC) at conical intersections (CI).^[39] In CIs, the degenerate overlap of the ground and excited state potential energy surfaces facilitates transitions through non-adiabatic

couplings, leading to high k_{nr} values. In a notable contribution by Crespo-Otero et al., they emphasized the control of the accessibility of conical intersections (CCIA) by increasing their energetical position as one of the key aspects for successful radiative relaxation.^[40]

4. Design Concepts

4.1. Previous concepts

Since the eminent article on “dual-state efficient” compounds became available in 2015, efforts from diverse scientists worldwide were conducted, reporting new scaffolds and ideas to realize efficient emission.^[4] In the first attempt at research advancement, Kumar et al.^[41] proposed three aspects for SSSE: (i) planarized structure, (ii) rigidified conformation, and (iii) prevention of π - π stacking. SSSEs must possess sufficient conjugation by incorporating molecular stiffness that restricts intramolecular motions and simultaneously allows torsional conformations in the solid-state to prevent aggregation quenching. Additionally, a D-A implementation can be used for ICT processes and emission tuning by push-pull effects. This balance coins a fusion of ACQ- and AIE-properties, and thus the term “bridging a gap” is frequently used to underline the potential of SSSEs.^[42]

4.2. A new perspective - classic versus non-classic SSSEs

In this contribution, we want to offer a different perspective on classifying SSSEs (Figure 2). Based on the current state of research, two main categories must be distinguished: (i) the classic combining build-up and (ii) a non-classical, modern origin for SSSE (Figure 2).

In the classic approach, subunits known for showing ACQ or AIE are combined with desired attributes to achieve the

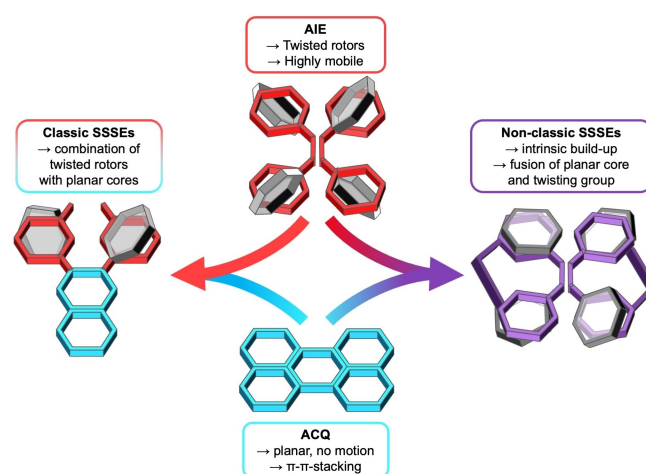


Figure 2. Molecular design of SSSEs: classic way (left) by combining AIE-motives (top) with planar ACQ-structures (bottom) and non-classic approach (right) by fusion of planar core with twisting groups.

opposing (AIE or ACQ) effect. The hitherto published luminophores classifiable as SSSEs are, in most instances, build-up by a combination of central core aromatics with moveable peripheral moieties that form twisted, rigid structures. For this, the corresponding authors shifted their attention to molecular scaffolds that can provide these desired features. However, the imagined connection needs to be conducted carefully, as just covalently attaching perylene with TPE results solely in the AIE effect due to unrestricted movement in solution.^[43]

Therefore, non-radiative dissipation in the solid-state must be suppressed in the case of compounds exhibiting ACQ. For this, voluminous peripheral groups can be attached to prevent detrimental excimer formation. For compounds displaying AIE, on the other hand, the mobility of rotating or vibrating subunits must be partially reduced, ideally to the extent of hindered but not prohibited movement, and at the same time preserve a molecular twist. For this purpose, stators are usually introduced, increasing the structure's rigidity without significantly limiting the emission capabilities in the solid-state. In summary, the main concept of a classic SSSE consists of the linkage of static and rotatable segments as a hybrid material.

In contrast to the attachment of static and rotatable segments, the non-classic approach provides the fusion into a single motif so that differentiation between those formerly split sections is not evident. This can be implemented by a planar core motif with subtle moveable groups that can rotate or vibrate slowly, adapt twisted conformations, or display stacking-averting molecular orientations by specific intermolecular interactions.

4.3. Criteria selecting SSSEs

This minireview intends to discuss qualitative structural characteristics rather than providing a complete literature summary of published compounds. Despite the diversified attempts to transform compounds in SSSEs, we will concentrate on molecular strategies focusing on intra- and intermolecular forces. In terms of discussing proper examples, we will specify several conditions that should serve as criteria to categorize selected compounds as SSSEs in this context. No unambiguous definition for the classification of SSSEs has yet been provided. Especially reports of compounds with major imbalances regarding their Φ_F values in solution and the solid-state raise issues, i.e. luminophores with low but not insignificant Φ_F in solution and high Φ_F in the solid-state are often denoted as “aggregation-induced emission enhancers” (AEE or AIEE).^[44] So far, to our best knowledge, no absolute definition regarding the sharp transition from AIEE to SSSE nor a uniform designation or nomenclature of these materials exists. Since no general known denotation of the opposing effect has been established, we will refer to compounds showing intense emission in solution but reduced Φ_F in the solid-state as an “aggregation-caused emission weakener” (ACEW).

Observed Φ_F must be significant enough to describe an SSSE as an efficient luminophore. However, many reports on emissive compounds did not further elaborate on photo-

physical properties in both aggregate states. Therefore, we solely focused on reported Φ_F both in solution and the solid-state, despite being aware that the number of true SSSEs is presumably much higher than estimated. For this, we chose compounds with Φ_F values higher than 0.05 in both states, although lower-emissive compounds still have great potential and established applications. In this regard, luminophores displaying efficient solution and solid-state emission shall provide balanced values for their respective Φ_F values. Compounds with a negligible Φ_F in one state or a too large difference between both states should instead be designated as enhancers or weakeners of either AIE or ACQ. Keeping these ambiguities mentioned above in mind, we propose a graphical mapping of SSSEs with the following conceptual illustration shown in Figure 3.

It is evident that the SSSE chart allows a larger tolerance area for emitters showing higher absolute Φ_F values than for low-emitting compounds. Although inorganic and polymeric materials and coordination complexes such as boron-dipyrromethene systems (BODIPYs) also possess interesting properties, no contributions featuring emitters classifiable as such will be discussed. Because this minireview aims to provide key molecular aspects, we concentrated on single monomeric molecules with a molecular weight M_w less than 2000 g/mol. Moreover, only examples emitting from excited singlet states will be discussed. Lastly, it must be stated that in some contributions, no information is provided regarding quantum yield values in either state and hence they are omitted in this minireview.

5. The Classic Approach to SSSEs

The classic way to develop novel SSSEs is the connection of static scaffolds with moveable subunits. A simple illustration of this concept is the straightforward approach by Strassert and co-workers.^[7] They designed novel D-A SSSEs by connecting planar naphthalonitriles (NCN) with *para*-substituted phenyl rotors (Figure 4). The phenyl groups rigidify the structure by extending the conjugation length, while their *ortho*-positioning

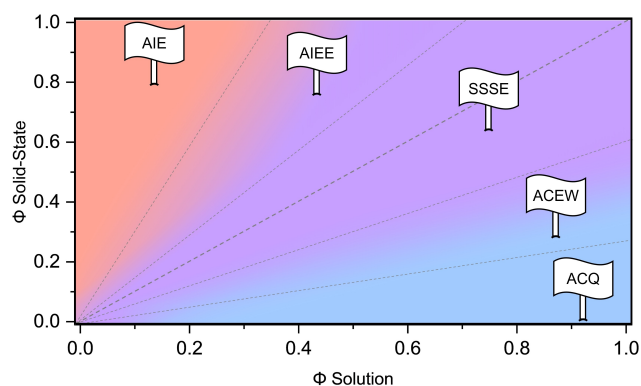


Figure 3. Conceptual illustration of the different luminescent domains AIE and ACQ transitioning over AIEE and ACEW to SSSE based on their state-dependent quantum yields.

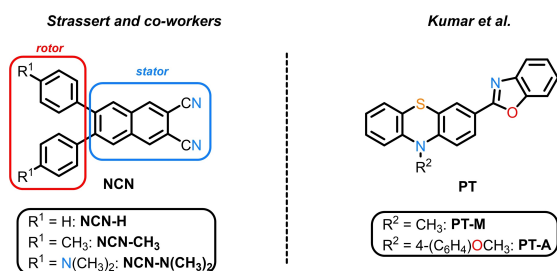


Figure 4. Chemical structures of NCN derivatives by Strassert and co-workers^[7] (left) and PT compounds from Kumar et al.^[41] (right).

inhibits full rotation. The expected asymmetrically twisted conformations were verified by crystal structure analysis for simple phenyl-compound NCN-H. Here, intermolecular C—H...N hydrogen bonds rigidified the system by generating one-dimensional chain-like patterns. In contrast, the absence of intermolecular π - π stacking interactions ultimately confirmed the origin of emissive behaviour in the solid-state (s-s). In aggregation studies, all investigated compounds revealed SSSE behaviour with approximately balanced Φ_F values (Table 1). Lastly, general trends regarding substituent effects were observed, such as bathochromic emission shifts upon increasing π -donor-strength of substituents or boosted Φ_F values by enhanced sterical hindrance.

The previously mentioned proposed design concepts by Kumar et al. were directly applied in their own attempt to develop novel SSSEs based on planar D-A systems.^[41] Oxazole and phenothiazine were chosen as the acceptor and donor units, respectively. Although a significant solid-state emission increase from 0.03 for methyl-compound PT-M to 0.33 upon attachment of a rotatable anisole group (PT-A) as a stacking modulator was achieved, the vast difference to the high solution quantum yields of 0.70 (PT-M) and 0.90 (PT-A) suggests a classification into ACEW rather than SSSE. Nevertheless, their contributed work deepened the knowledge of indispensable criteria when designing emitters in both states, again revealing the classic connection of rotor and stator.

5.1. Triphenylamine derivatives

One of the most prominent motifs used in literature to synthesize novel compounds exhibiting remarkable emissive

properties is the propeller-shaped triphenylamine (TPA) (Figure 5). Unlike its hydrogen derivative NH₃, the average C—N—C bonding angle of 119.6° is close to a perfect threefold-symmetric arrangement, thus in trigonal pyramidal geometry with a planar central nitrogen atom.^[45] Full rotation of the peripheral rotors is sterically impaired, resulting in emissive behaviour in solution and causing twisted structures preventing close-contact interactions in the crystalline state.^[46] Therefore, it is often overlooked in literature reports that a certain controversy exists because TPA itself exhibits balanced emissions in both states with Φ_F values of 0.10 in THF and 0.13 in the crystalline state (Table 2).^[4] Hence, it is debatable whether reported SSSEs based on TPA motifs are attempts for efficiency optimization and emission tuning rather than novel developed concepts. Nonetheless, TPA derivatives can be considered the prototype traditional SSSE scaffold since rotors are attached to a rigid, planar core.^[47]

In 2007, Patra et al. reported interesting emissive properties of the *para*-nitrile substituted derivative tris(4-cyanophenyl)amine TCPA.^[48] With the implemented D- π -A core, balanced quantum yield values were obtained in both THF ($\Phi_F = 0.30$) and the solid-state ($\Phi_F = 0.42$). In contrast to an expected non-dipolar D₃-symmetry, C₂-symmetry is displayed in the crystal structure, influencing the molecular charge polarization and thus corresponding dipole moments. Both *H*-type and *J*-type dimer units were observed in the crystal lattice, explaining the trends of observed small Stokes-shifts and dual-emission in the solid-state. Therefore, supramolecular interactions account for the emission in the condensed solid-state.

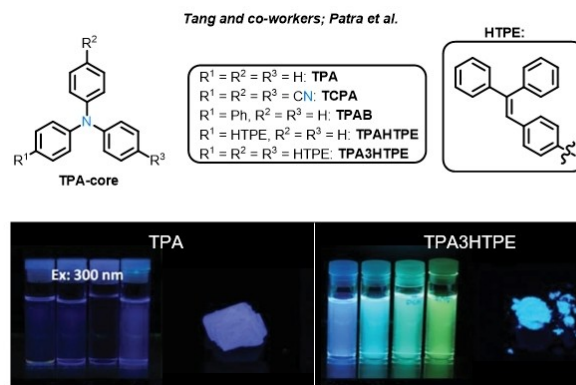


Figure 5. Chemical structures of TPA derivatives (top) and photographs of TPA ($\lambda_{Exc} = 300$ nm) and TPA3HTPE ($\lambda_{Exc} = 365$ nm) in solution (10^{-5} M, from left to right: toluene, THF, DCM, DMF) and the crystalline state. Adapted and reproduced with permission from Wiley-VCH, copyright 2015.^[4]

	λ_{em}^{S-S} [nm]/ Φ_F	λ_{em}^{Sol} [nm]/ Φ_F	Ref.
NCN-H	428/0.11 ^[a]	400/0.15 ^[b]	[7]
NCN-CH ₃	428/0.32 ^[a]	407/0.22 ^[b]	[7]
NCN-N(CH ₃) ₂	560/0.20 ^[a]	566/0.36 ^[b]	[7]
PT-M	~480/0.03 ^[c]	~515/0.70 ^[d]	[41]
PT-A	~515/0.33 ^[c]	~515/0.90 ^[d]	[41]

[a] = 10 μ M, THF/H₂O = 1/99; [b] = 10 μ M, THF; [c] = not specified; [d] = DMSO (unknown conc.); ~ = graphically extracted.

	λ_{em}^{S-S} [nm]/ Φ_F	λ_{em}^{Sol} [nm]/ Φ_F	Ref.
TPA	380/0.10 ^[a]	357/0.13 ^[b]	[4]
TCPA	414/0.42 ^[c]	380/0.30 ^[d]	[48]
TPAB	397/0.18 ^[a]	398/0.35 ^[b]	[4]
TPAHTPE	448/0.87 ^[a]	482/0.47 ^[b]	[4]
TPA3HTPE	455/0.55 ^[a]	484/0.73 ^[b]	[4]

[a] = crystalline state; [b] = 5 μ M, THF; [c] = thin film; [d] = 0.27 μ M, THF.

Time-dependent density functional theory (TD-DFT) calculations supported the assumption that impeded torsional motion of the phenyl groups increase lattice rigidity and lessen non-radiative vibrational relaxation.

Partially rigidified conformations of TPA-derived luminophores were further investigated in the previously mentioned communication by Tang and co-workers in 2015, which is often considered the beginning of SSSE research.^[4] In this approach, the effect of increased π -electronic systems was studied with biphenyl-derivative (TPAB) and triphenylethylene-linked (HTPE) mono- (TPAHTPE) and tri-substituted (TPA3HTPE) structures. Generally, the extended conjugation planarized and thus rigidified the molecular conformations in solution compared to TPA, as evident by Φ_F data (Table 2). This effect was termed *conjugation-induced rigidity* (CIR). It provides a method for boosting emission in solution while distorting the molecular orientation in the crystal lattices, which mitigates detrimental close-contact interactions such as *H*-type excitons. For TPA3HTPE, however, it is assumed that the overly increased conjugation impedes distortion and twisting in the solid-state, hence resulting in more unbalanced Φ_F values. Also, a pivotal emphasis should be laid on the correct substitution pattern because the exchange of vinyl-proton with another phenyl ring or nitrile group leads to detrimental motional emission quenching in solution, demoting the systems to AIE behaviour.

The applicability of CIR was verified in several literature reports, although only in a few cases balanced Φ_F values were obtained. Interestingly, a single bond locking two phenyl rings leads to carbazole (Cz) motifs, which are also widely used because of their impressive emissive characteristics and are somewhat of a sister system to TPA.^[49]

5.2. Chromophore isolation

Another proposed and already widely approved strategy to surmount the ACQ effect is possible by attaching peripheral bulky alkyl chains on an emissive core to prevent stacking interactions by sterically shielding. Meng and co-workers termed this concept “*self-isolation enhanced emission*” (SIEE) and showcased it on a series of benzo[1,2,5]-thiadiazole (DBBT) derivatives with spaced phenyl rings, establishing CIR and increasing chain length (DBBT-C0, C4, C8, and C12).^[50] For all luminophores, Φ_F values above 0.90 were measured in solution, emphasizing the impressive emissive scaffold chosen in this study. In the solid-state, only compounds DBBT-C4 and DBBT-C8 achieve almost equal Φ_F values, whereas the moderate Φ_F values of compounds DBBT-C0 and DBBT-C12 instead suggest a classification as an ACEW. To obtain SSSEs based on the SIEE concept, a careful medium-sized spacer must thus be selected to maintain the balance of sufficient aloofness and non-exaggerated internal conversion possibilities (Figure 6).

With the SIEE concept established, attention was drawn to transforming well-known highly emissive scaffolds in solution suffering from the ACQ-effect into SSSEs by attaching voluminous substituents (Figure 7).^[51] In this regard, especially perylene bisimides (PBIs) are known for high molar absorptivity,

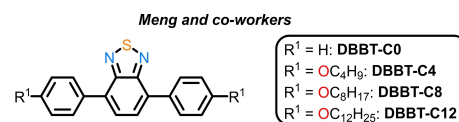


Figure 6. Chemical structures of DBBT derivatives.^[50]

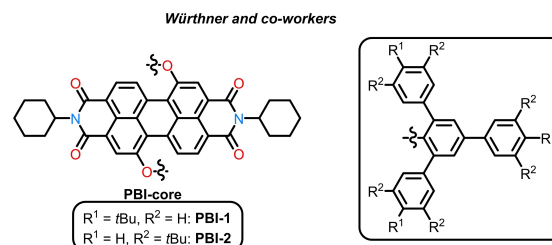


Figure 7. Chemical structures of PBI derivatives.^[53,54]

lightfastness, and chemical stability, as well as high quantum yields in solution.^[52] However, they are generally non-emissive in the solid-state because of the ACQ effect. Nonetheless, Würthner's group managed to optimize the SIEE concept, reaching the SSSE tip of the iceberg with PBI-1, displaying one of the highest combined Φ_F values in both solution and the solid-state close to unity.^[53] In their contribution, intramolecular enclosing was envisioned to prevent π - π stacking by distance-keeping with bulky tris-phenoxy substituents. Crystal structure analysis revealed their opposed bending, thus isolating the PBI core from the surrounding environment with large chromophore-to-chromophore distances of 8.1 Å. This design concept thus synthetically mimics the build-up of the emissive chromophore in the green-fluorescent protein (GFP). However, it must be stated that the solid-state Φ_F value given in Table 3 is the value after correction for reabsorption processes, which can generally lead to falsified data.

In a consecutive investigation, voluminous substituents' influence on increased sterical demand was studied.^[54] Despite achieving a considerable interplanar distance of 15.7 Å with PBI-2, the solid-state's uncorrected quantum yield values of around 0.60 would suggest an ACEW classification.

Table 3. Photophysical properties of DBBT and PBI derivatives.

	$\lambda_{\text{em}}^{\text{S-S}}$ [nm]/ Φ_F	$\lambda_{\text{em}}^{\text{Sol}}$ [nm]/ Φ_F	Ref.
DBBT-C0	~480/0.42 ^[a]	~487/0.95 ^[b]	[50]
DBBT-C4	~540/0.71 ^[a]	~545/0.98 ^[b]	[50]
DBBT-C8	~510/0.78 ^[a]	~546/1.00 ^[b]	[50]
DBBT-C12	~517/0.44 ^[a]	~546/0.92 ^[b]	[50]
PBI-1	565/> 0.90 ^[c]	581/1.00 ^[d]	[53]
PBI-2	570/0.60 ^[e]	575/1.00 ^[d]	[54]

[a] = amorphous powder; [b] = THF (unknown conc.); [c] = crystalline state, corrected value; [d] = 0.2 μM , DCM; [e] = polycrystalline powder; ~ = graphically extracted.

5.3. Positional dependency of rotor-stator connection

Dong's group investigated the transformation of polyarylpyrrole luminophores into SSSEs in several consecutive reports. First, the influence of phenyl substitution position was studied.^[55] The authors deduced that phenyl groups in 2,5-position provide extended conjugation area and are thus vital luminogenic parts for emissive behaviour in the visible spectrum. Substituents in the 3,4-position, on the other hand, are more spatially separated and responsible for providing twisted conformations in the solid-state, as confirmed by crystal structure analysis. A phenyl ring in 1-position on the nitrogen atom exhibits a high degree of rotational freedom and therefore allows for non-radiative decay in solution. With this information in hand, the combined 2,3,4,5-tetraphenyl-1*H*-pyrrole **TePP** demonstrated SSSE properties, whereas compounds with different substitution patterns displayed ACQ (**TPP-1,2,5**) or AIE (**TPP-1,3,4**). Interestingly, **TePP** shows balanced quantum yields in solution and the solid-state as well as only small emissive changes upon temperature or viscosity increase, evidencing the independency of the molecular surrounding (Table 4).

The following report presented the facile conversion of ACQ-core **TPP-1,2,5** in SSSEs.^[56] In contrast to the previously established requirement of 3,4-substitution for solid-state emission, twisted conformations were achieved by attached 2,5-biphenyl-arms bearing different electron-withdrawing (i.e.

	$\lambda_{\text{em}}^{\text{S-S}}$ [nm]/ Φ_F	$\lambda_{\text{em}}^{\text{Sol}}$ [nm]/ Φ_F	Ref.
TPP-1,2,5	385/0.02 ^[a]	385/0.10 ^[b]	[55]
TePP	403/0.74 ^[a]	399/0.66 ^[b]	[55]
TPP-1,3,4	382/0.13 ^[a]	345/0.02 ^[b]	[55]
TPP-1,2,5-CHO	501/0.64 ^[c]	499/0.85 ^[b]	[56]
TPP-1,2,5-OCH₃	439/0.52 ^[d]	424/0.69 ^[b]	[56]
TPP-1,3,4-C₃H₇	391/0.45 ^[e]	365/0.44 ^[b]	[57]
TPP-1,3,4-OCH₃	393/0.47 ^[e]	367/0.44 ^[b]	[57]
TPP-1,3,4-CN	423/0.44 ^[e]	425/0.56 ^[b]	[57]

[a] = crystalline state; [b] = 10 μM , THF; [c] = amorphous powder; [d] = after recrystallization; [e] = not specified.

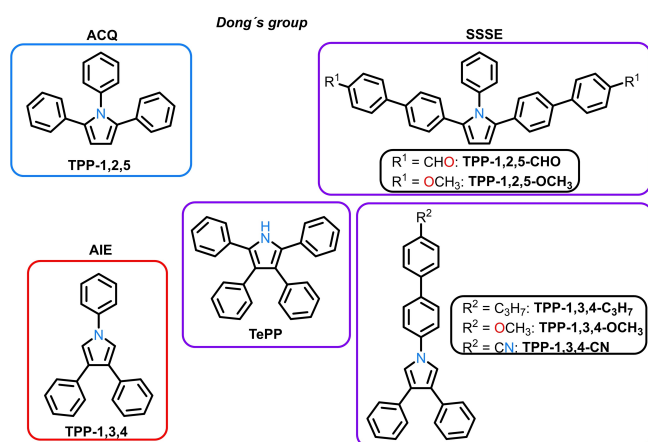


Figure 8. Chemical structures of pyrrole derivatives.^[55–57]

CHO) or electron-donating groups (i.e. OCH₃) (Figure 8). Despite overall high Φ_F values in solution were obtained, only aldehyde-compound **TPP-1,2,5-CHO** and methoxy-compound **TPP-1,2,5-OCH₃** display moderate solid-state Φ_F and are thus qualifiable as an SSSE. It must be mentioned that the solid-state Φ_F of **TPP-1,2,5-CHO** reaches high values not as an amorphous powder but only after recrystallization, exhibiting *crystallization-induced emission enhancement* (CIEE).

In their last report, the rotational quenching of phenyl-substitution in 1-position was successfully inhibited by a volume increase of the attached aromatic subunit, thus reducing intramolecular motion.^[57] For this purpose, the established biphenyl-system equipped with nitrile, methoxy, or alkyl chain groups in 4-position was coupled with previously AIE-active **TPP-1,3,4**. Surprisingly, no positional influence of phenyl substituents was observed, as all investigated compounds display SSSE characteristics with moderate Φ_F values between 0.30–0.56 in both states. Interesting variable-temperature experiments revealed an unexpected emission intensity increase for several luminophores in solution upon heating, which was explained by enhanced molecular rigidification through planarization.

In 2018, Wang et al. studied subtle variations regarding the position and chalcogen atom of diarylmaleimides (**DAM**) with 2- or 3-substituted benzofuran (**M2O**, **M3O**) and benzothiophene (**M2S**, **M3S**) moieties (Figure 9).^[58] Interestingly, both oxygen derivatives showed good SSSE behaviour, whereas emission of sulfur derivatives was quenched either in solution for **M2S** (AIE) or the solid-state for **M3S** (ACQ). The origins of the distinct emissive properties were investigated with crystal structure analyses and DFT calculations. Structural distortions are generally higher for the benzothiophene derivatives and more prominent for 3-connected compounds, explaining the superior Φ_F values compared to **M2O** and **M2S** through more twisted conformations. **M2O** still shows emission in solution due to partial rigidification by intramolecular hydrogen bonding of maleimide oxygen atom. Upon aggregation, emission of **M2S** arises due to JAF, while weak *H*-aggregation of **M2O** still allows significant radiative decay.

The interesting properties of the diarylmaleimide core led to further investigations. Eisler's group varied several sulfur-containing heterocycles with a slightly modified **DAM** scaffold but turned the 3-substituted benzothiophene **DAM-C3** into an

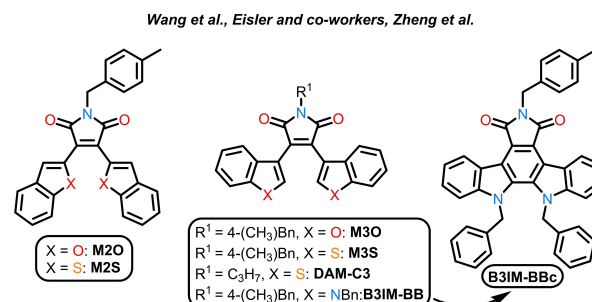


Figure 9. Chemical structures of DAM derivatives.^[58–60]

impressive SSSE (Table 5).^[59] Zheng et al. extended the DAM research by photocyclization of indole derivatives such as B3IM-BB to closed structures (B3IM-BBc), further synthesizing compounds classifiable as SSSEs.^[60]

Finally, excited state intramolecular proton transfer (ESIPT) is another excellent concept illustrating the positional dependency of rigidifying moieties.^[61] In this regard, Huang et al. envisioned a balance between rotation and conjugation of thiazolo[5,3-*b*]thieno-[3,2-*e*]pyridine derivatives (DF) (Figure 10).^[42] The molecular build-up consists of five aromatic cycles with a centered stator and three peripheral rotors. Influence of proton-bearing substituents was studied by modification of ring D. As a reference compound, substance DF0 with 4-substituted hydroxy-group shows low Φ_F values in solution and solid-state, as both rotational quenching and π - π stacking facilitate non-radiative decay (Table 6). However, attaching the hydroxy-group in the *ortho*-position restricted rings C and D, thus inducing emission in H-bond donating solvents like DMSO and DMF as well as in the solid-state due to head-to-tail JAF (compound DF1). In an attempt to change the acidity of the bridged proton, aniline derivatives DF3 and DF5 were investigated. Although reaching expectedly higher Φ_F

values in solution, DF3 displays classic ACQ behaviour as no JAF was observed. In contrast, the more sterically shielded analogue DF5 with a 4-methylbenzenesulfonyl-substituent was able to both successfully rigidify the molecular conformation in solution and maintain intermolecular spacing in the solid-state. Here, another weak H-bonding between the aromatic proton of ring E and the oxygen atom of the sulfonyl group enhanced intramolecular twisting. Furthermore, distorted J-aggregation decreased intracavity π - π stacking, resulting in intense solid-state emission.

In a further attempt, apart from proton transfer, the influence of extended π -elongation was studied by nitrile substitution in *ortho*-position leading to compound DF2. Although considerable Φ_F values were measured, the considerable imbalance suggests an ACEW classification. However, a drawback of the ESIPT concept must be stated, since Φ_F values of ESIPT-active luminophores are immensely dependent on solvent acidity and specific solvent-solute interactions and thus not entirely classifiable as unconstrained SSSEs.

Therefore, this concept showed that by controlling the position, acidity, and molecular surroundings necessary for H-bonding, significant differences in the emissive behaviour of luminophores can be induced without drastically changing the number of existing mobile and static segments. For further information on ESIPT-active SSSEs, we refer to the recently published comprehensive review of Stoerkler et al.^[62]

6. The Non-Classic Approach to SSSEs

6.1. Tetraphenylethylene derivatives

Similar to the prominent usage of the TPA motif in classic SSSEs, many reports of non-classic SSSEs incorporated the tetraphenylethylene (TPE) subunit in their molecular design. The four independent phenyl rings can rotate nearly without restraint around the central planar double bond.^[63,64] This rotation results in an almost non-emissive behaviour in solution but upon aggregation, the RIM effect leads to enhanced blue-light emission with a Φ_F value of 0.25.^[19]

In an investigation attempt to better understand the RIM mechanism, Tang and collaborators accomplished to impede the phenyl ring rotation through oxygen bridging in compounds 1OTPE and 2OTPE (Figure 11).^[65] Whereas low Φ_F values were observed for the monoether-bridged 1OTPE, an emissive increase in both solution and the solid-state with balanced results was observed for the diether-bridged derivative 2OTPE (Table 7). These implemented ether-bridges successfully suppress rotational motion in solution but allow vibrations leading to twisted conformations in the solid-state that avert detrimental quenching through stacking, excellently illustrating the fusion of rotor and stator into one structural element without clear spatial distinction.

Besides the covalent motion annihilation, sterically repulsion is another possibility of movement restriction. Zhang et al. elaborated that simple *ortho*-substituted methyl groups suffice to impede motion (Figure 12).^[66] Like in the aforementioned

Table 5. Photophysical properties of DAM derivatives.

	$\lambda_{\text{em}}^{\text{S-S}}$ [nm]/ Φ_F	$\lambda_{\text{em}}^{\text{Sol}}$ [nm]/ Φ_F	Ref.
M2O	630/0.46 ^[a]	555/0.47 ^[b]	[58]
M2S	620/0.14 ^[a]	573/0.02 ^[b]	[58]
M3O	557/0.58 ^[a]	506/0.71 ^[b]	[58]
M3S	599/0.05 ^[a]	530/0.85 ^[b]	[58]
DAM-C3	601/0.87 ^[a]	548/0.80 ^[c]	[59]
B3IM-BB	650/0.14 ^[a]	587/0.29 ^[d]	[60]
B3IM-BBc	525/0.41 ^[a]	492/0.56 ^[d]	[60]

[a] = not specified; [b] = THF (unknown conc.); [c] = chloroform (unknown conc.); amorphous powder; [d] = 10 μ M, THF.

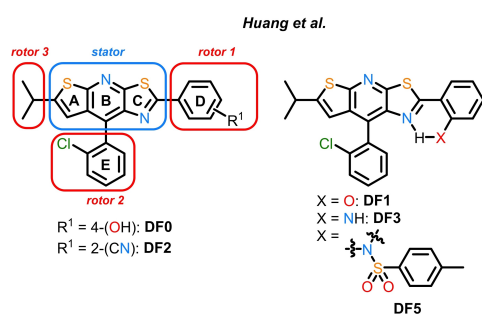


Figure 10. Chemical structures of derivatives showing ESIPT.^[42]

Table 6. Photophysical properties of ESIPT derivatives.

	$\lambda_{\text{em}}^{\text{S-S}}$ [nm]/ Φ_F	$\lambda_{\text{em}}^{\text{Sol}}$ [nm]/ Φ_F	Ref.
DF0	451/0.01 ^[a]	588/0.00 ^[b]	[42]
DF1	550/0.26 ^[a]	568/0.24 ^[b]	[42]
DF2	564/0.40 ^[a]	495/0.90 ^[b]	[42]
DF3	525/0.02 ^[a]	490/0.48 ^[b]	[42]
DF5	571/0.51 ^[a]	588/0.74 ^[b]	[42]

[a] = not specified; [b] = 20 μ M, DMSO.

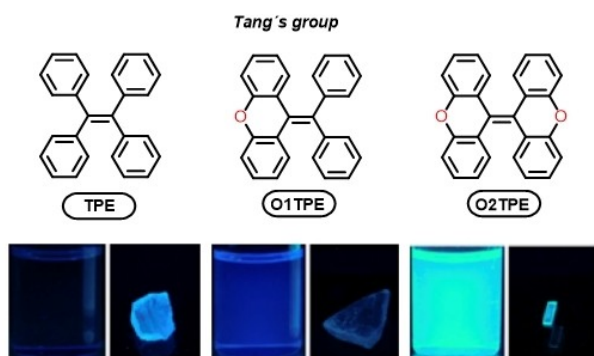


Figure 11. Chemical structures of **TPE** and bridged derivatives **O1TPE** and **O2TPE** (top) and corresponding photographs ($\lambda_{\text{Exc}} = 350 \text{ nm}$) in THF (10^{-5} M) and the crystalline state (bottom). Adapted and reproduced with permission from the Royal Society of Chemistry, copyright 2012.^[65]

Table 7. Photophysical properties of TPE derivatives.			
	$\lambda_{\text{em}}^{\text{S-S}}$ [nm]/ Φ_F	$\lambda_{\text{em}}^{\text{Sol}}$ [nm]/ Φ_F	Ref.
TPE	453/0.24 ^[a]	n.d./n.d.	[65]
O1TPE	458/0.08 ^[a]	401/0.05 ^[b]	[65]
O2TPE	467/0.31 ^[a]	466/0.30 ^[b]	[65]
DMTPE	417/0.21 ^[c]	n.d./<0.01 ^[b]	[66]
TMTPE	429/0.96 ^[c]	481/0.64 ^[b]	[66]
C1TPE	475/0.22 ^[c]	508/0.24 ^[b*]	[67]
C2TPE	459/0.51 ^[c]	527/0.49 ^[b*]	[67]
C3TPE	484/0.80 ^[c]	492/0.97 ^[b*]	[67]
TPE-3-model	487/0.64 ^[d]	513/0.03 ^[e]	[68]
TPE-3-stack	506/0.83 ^[d]	501/0.82 ^[e]	[68]

[a] = crystalline; [b] = 10 μM , THF (* = 100 μM); [c] = aggregate in THF/H₂O 5/95 (100 μM); [d] = film; [e] = 10 μM , DMSO; n.d. = not determined.

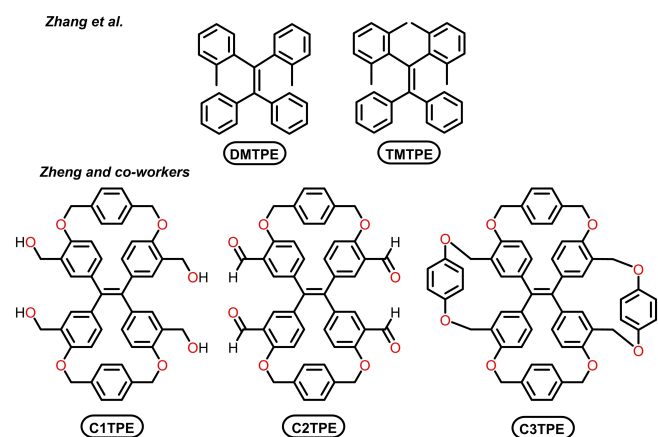


Figure 12. Chemical structures of methyl-substituted derivatives **DMTPE** and **TMTPE** (top) and cyclized derivatives **C1TPE** to **C3TPE** (bottom).^[66,67]

bridged ether series, the hindrance effect was studied with a close but still inadequate restricting compound, dimethyltetraphenylethylene (**DMTPE**), and the further developed and thus sufficient regulating tetramethyltetraphenylethylene (**TMTPE**). Whereas the two methyl groups of **DMTPE** are still not enough to induce emission in solution, **TMTPE** shows impressive high Φ_F values in both states (Table 7). Following

crystallization, the respective analysis of **TMTPE** revealed a symmetry-disordered structure by the four-fold axis without noticeable $\pi\cdots\pi$ or C—H $\cdots\pi$ interactions, confirming that the loose packing is responsible for the luminescence properties.

Zheng and co-workers presented another TPE-rigidification approach via linkage in their series of cyclized benzyl ether derivatives **C1TPE**, **C2TPE**, and **C3TPE** (Figure 12).^[67] With an intrinsically twisted connected cycle in **C3TPE**, exceedingly high Φ_F values of 0.80 in the solid-state and 0.97 in THF were achieved, further proofing the RIR mechanism. Interestingly, the aldehyde and benzyl alcohol precursors also display balanced Φ_F values, however, significantly decreased upon reduction from **C1TPE** to **C2TPE**. Although crystal structure analyses of **C1TPE** and **C3TPE** revealed distorted conformations with adopted *cis*-positioning of the cycles that prevent π - π interactions, the benzyl ether connections ensure the necessary molecular flexibility for sufficient conjugation, as evident by the Φ_F values in solution. Apart from this, the same tendency can again be noticed as in the other examples previously. Therefore, the conclusion can be drawn that an increase in the emission intensity in both states can consistently be observed with an increased number of interlocked phenyl rings and an increase in stiffness or reduction of mobility while maintaining a twisted structure.

In a final TPE-featured example, Zheng et al. reported interesting properties of purely organic cages based on dynamic covalent chemistry (DCC) with imines.^[68] Starting with a corresponding aldehyde precursor (not investigated and thus not shown), acid-catalyzed formation of the desired **TPE-3-stack** and reference compound **TPE-3-model** yielded once again a systematic study of three comparable luminophores (Figure 13). **TPE-3-model** displays expected AIE characteristics because of the unhindered motional quenching in solution, whereas **TPE-3-stack** shows high and balanced Φ_F values in solution and the solid-state (Table 7). Elaboration via DFT-optimized structures suggested an interplane distance of 5.4 Å for the central double-bond. Indifferent behaviour in variable-temperature NMR studies further confirmed the assumed high rigidity of the system, explaining the remarkable luminescence properties. Therefore, all reports showed that TPE is suitable as a basis for

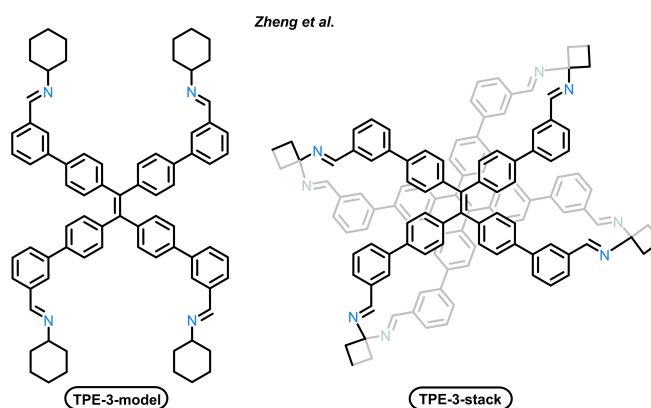


Figure 13. Chemical structures of **TPE-3-model** and **TPE-3-stack**.^[68]

designing novel non-classic SSSEs, requiring only minor modifications to restrict the mobility of peripheral ring rotations through bridging, linking, or sterically inhibition.

6.2. Intrinsically twisted motifs

Several miscellaneous subunits feature intrinsically twisted conformations and are thus suitable for developing novel SSSEs. An intriguing approach was pursued by Oyama et al. with their dimethylsila[7]helicene (**Heli-1**, Figure 14).^[69] The large atomic diameter of silicon leads to a total dihedral angle-sum of 99.5° and therefore generates a largely distorted structure, achieving balanced values for Φ_F (Table 8).

Chen and co-workers reported emissive properties of phthalimide-luminophores based on a tetrahydro[5]helicene core.^[70] Although a torsion angle of 54.0° was observed in the crystal structure of **Heli-2**, the smaller conjugation length compared to **Heli-1** led to low emissive behaviour in solution ($\Phi_F = 0.05$) but maintained acceptable in the solid-state ($\Phi_F = 0.26$). Therefore, increased conjugation area was deduced to enhance the transition dipole moment of the S_1 state, which facilitates radiative decay in solution. Additionally, elongated phenyl rings reduce the reorganization energy and the Duschinsky rotation effect, which results in a decrease of IC rates and thus an increase of the molecular rigidity.^[71] Arylation was performed using *para*-positioned substituents with different electronic properties. The resulting compounds **Heli-3-5** were expectedly able to emit more efficiently in solution (Table 8). However, it must be stated that due to the applied CIR effect, these compounds technically classify as classic SSSEs

because of their spatial separation of stator and rotor segments. Nevertheless, the helicene subunit marks a distinctive core motif with remarkable intrinsically twisted characteristics.^[72] Based on their results, the group reported a library of further developed SSSEs with varied peripheral aromatic rotors, which shall not be further discussed in the scope of this minireview.^[73]

So far, in all the compounds shown previously, a trend of multiple aromatic systems linked by bonds has consistently been shown to create an adequately sized conjugated π -system responsible for the respective photophysical properties.^[76] In a pioneering work, Katagiri's group investigated the reduction of unnecessary phenyl rings to the absolute minimum in their report of tetra-substituted single-benzene luminophore **BMeS-p-A** (Figure 14).^[74] A strong intramolecular push-pull effect had to be applied to ensure emissive properties in the visible spectrum.^[77] For this, they chose amino and sulfonyl groups as strong D-A moieties in *ortho*-/*para*-positioning to form an X-shaped structure, respectively. This push-pull system is highly efficient and separates the highest occupied molecular orbital (HOMO) and lowest unoccupied molecular orbital (LUMO), evident by the energy gap of 4.04 eV for the absorption and 2.98 eV for the emission process. This leads to excellent photostability and efficient fluorescence in the blue range of the visible light without the otherwise necessary base of a relatively large π -system, which would have to be extended over multiple aromatic units.^[78]

Furthermore, this substitution pattern enabled molecular rigidification by strong intramolecular hydrogen bonding, resulting in green emission with high and balanced Φ_F values of 0.70 in DMSO and 0.69 in the solid-state (Table 8). The hydrogen bonding was further analyzed via crystal-structure analysis. The formation of stable six-membered rings accounted for adapted *syn*-configuration of the sulfonyl groups. Due to the resulting ladder structure in the solid-state, no π - π stacking occurs and thus enables emissive behaviour. Moreover, no environmental sensitivity like a pronounced decrease of Φ_F even in protic solvents such as water or methanol are observable, which are ascribed to the symmetrical structure and the associated non-existent difference in dipole moments between S_1 and S_0 . DFT calculations also suggested a deplanarization of the sulfonyl-group in respect to the benzene plane and of the nitrogen hybridization upon excitation, which was accounted responsible for the observed Stokes shift of around 100 nm in both states.

Because of other exceptional properties such as facile four step synthesis without the need for column purification, environmentally insensitive behaviour, and possible additional functionalization, this compound was further modified in later reports, i.e. with an attached dodecyl chain at the anilines for vesicle formation^[79] and therefore lipid droplets visualization.^[80]

Since Katagiri's report in 2015, many efforts have been made to design and investigate single-benzene-based fluorophores due to their small size and compact structure.^[81] Huang et al. also reported a similar tetra-substituted core with *ortho*-/*para*-positioning of D-A moieties, respectively (Figure 14).^[75] Interestingly, a small excited state dipole moment μ_e of 7.2 D was determined for **BMeC-p-DMA**, which explains the efficient

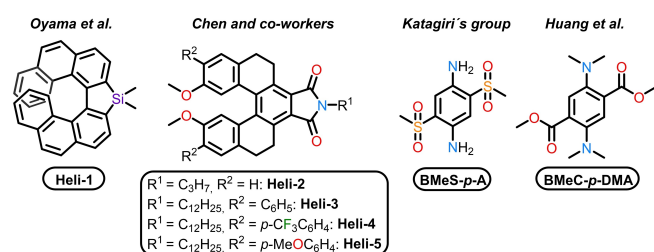


Figure 14. Chemical structures of helicene derivatives **Heli-1** to **Heli-5** and single-benzene luminophores **BMeS-p-A** and **BMeC-p-DMA**.^[69,70,74,75]

	λ_{em}^{S-S} [nm]/ Φ_F	λ_{em}^{Sol} [nm]/ Φ_F	Ref.
Heli-1	n.d./0.17 ^[a]	450/0.23 ^[b]	[69]
Heli-2	496/0.26 ^[c]	474/0.05 ^[d]	[70]
Heli-3	502/0.51 ^[c]	502/0.70 ^[d]	[70]
Heli-4	493/0.56 ^[c]	485/0.46 ^[d]	[70]
Heli-5	518/0.61 ^[c]	526/0.85 ^[d]	[70]
BMeS-p-A	477/0.69 ^[e]	509/0.70 ^[f]	[74]
BMeC-p-DMA	552/0.73 ^[g]	531/0.78 ^[h]	[75]

[a] = not specified; [b] = 4.2 μ M, DCM; [c] = film; [d] = 10 μ M, DCM; [e] = powder; [f] = 5 μ M, DMSO; [g] = crystalline; [h] = cyclohexane (unknown conc.); n.d. = not determined.

SSSE properties because of minimized dipole-dipole interactions and avoided π - π stacking (interplane distance of 5.8 Å). Intermolecular hydrogen bonds were again responsible for constraining free rotational and vibrational motions, as evident by crystal structure analysis.

6.3. SSSEs with terephthalonitrile-core

Recently, the emissive properties of luminophores with a *para*-terephthalonitrile (TN) core have inspired a lot of research. By facile nucleophilic aromatic substitution of commercially available tetra-substituted halogen derivatives, many pentacene-derived luminophores are quickly accessible and therefore tunable.

Voskuhl and co-workers reported chalcogen bridged ethers in a series of eight compounds and investigated the influence of chalcogen exchange by positioning and quantity (Figure 15).^[8] An increasing sulfur content generally leads to bathochromically shifted emission wavelengths and lower Φ_F values in solution because the spin-orbit coupling facilitating energetic deactivation crossing via intersystem-crossing is more probable (Table 9). Furthermore, sulfurs reduced electronegativity, increased atomic size, and different geometry causes a conjugation disturbance, leading to tilted non-planar structures. Although an almost planar structure is hence assumed for compound **O₄**, π - π stacking in the solid-state is averted due to the sterically crowded nitrile groups, which form pronounced supramolecular interactions because of their high polarizability. Therefore, **O₄** and **SO₃** represent the most efficient SSSEs with balanced values in the reported study since the interplaying conditions for solution (conjugation and planarity), and solid-state emission (flexibility and stacking prevention) are matched. It must be mentioned that no solvatochromic study was performed due to the generally low solubility of the com-

pounds, although increased Φ_F values are expected for the D-A-D structured parent motif in less polar solvents than DMF.

In a prior report by Feng and collaborators, the parallel-regioisomer of **S₂O₂-e-p** was isolated using a different starting material.^[82] In contrast, in Voskuhl's study, only the antiparallel-isomer (**S₂O₂-e-a**) was isolated and analyzed. Interestingly, both regioisomers showed different photophysical behaviour with **S₂O₂-e-a** showing polymorphism, which was investigated with crystal structure analysis. Here, the molecules in the yellow emissive polymorph were orthogonally arranged and exhibited multiple O... π and π ... π interactions. In contrast, more π ... π contacts were observed for the orange emissive polymorph in its slipped parallel stacking pattern, explaining the red-shifted emission.

Hiscock et al. studied the influence of main group change, instituting nitrogen as the bridging atom with several sulfur and oxygen variations.^[83] Unfortunately, only a few compounds were selected for photophysical analysis. Nevertheless, phenothiazine compound **SNO₂** displays relatively low but balanced Φ_F values, being classifiable as an SSSE. Due to the valency of nitrogen, an ethyl chain was used to saturate the structure. However, its low steric crowdedness allowed significant stacking interactions in the crystal structure, although **SNO₂** adopted a bent conformation.

7. Benchmarking of Selected SSSEs

After discussing several characteristics of various SSSEs, we would like to present a benchmarking chart classifying the discussed examples regarding their balanced Φ_F values in both states (Figure 16). As indicated before, currently no sharp definition exists for SSSEs, hence we suggest the usage of this comparative chart. In the case of exceedingly higher values in either case, the proper denotation should be emission weakening (ACEW) or enhancement (AIEE) upon entering the solid-state like phase, such as by thermal or viscous rigidification, aggregation or crystallization etc.

Regarding the listed quantum yields of the discussed emitters in this review, some luminophores like ACEW-classified **PT-A** display much higher total Φ_F values than lower-efficient compounds such as the SSSE-categorized **SO₃**. It is apparent that **PT-A** suffers from differently efficacious deactivation mechanisms in both states compared to **SO₃**, which shows a similar probability for emission in either state. However, because comparable non-radiative deactivation processes occur in both solution and the solid-state, the resulting emission is balanced. Therefore, in order to obtain balanced efficient emitters classifiable as SSSEs, knowledge about the concerned non-radiative deactivation pathways has to be established through elaborated syntheses and investigations of novel luminophores.

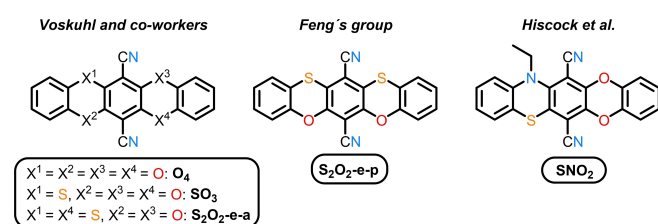


Figure 15. Chemical structures of TN derivatives.^[8,82,83]

	λ_{em}^{S-S} [nm]/ Φ_F	λ_{em}^{Sol} [nm]/ Φ_F	Ref.
O₄	498/0.20 ^[a]	481/0.32 ^[b]	[8]
SO₃	548/0.23 ^[a]	530/0.33 ^[b]	[8]
S₂O₂-e-a	593/0.07 ^[a]	537/0.27 ^[b]	[8]
S₂O₂-e-p	580/0.13 ^[a]	518/0.38 ^[c]	[82]
SNO₂	585/0.13 ^[d]	580/0.23 ^[e]	[83]

[a] = powder; [b] = DMF (unknown conc.); [c] = THF (unknown conc.); [d] = film; [e] = chloroform (unknown conc.).

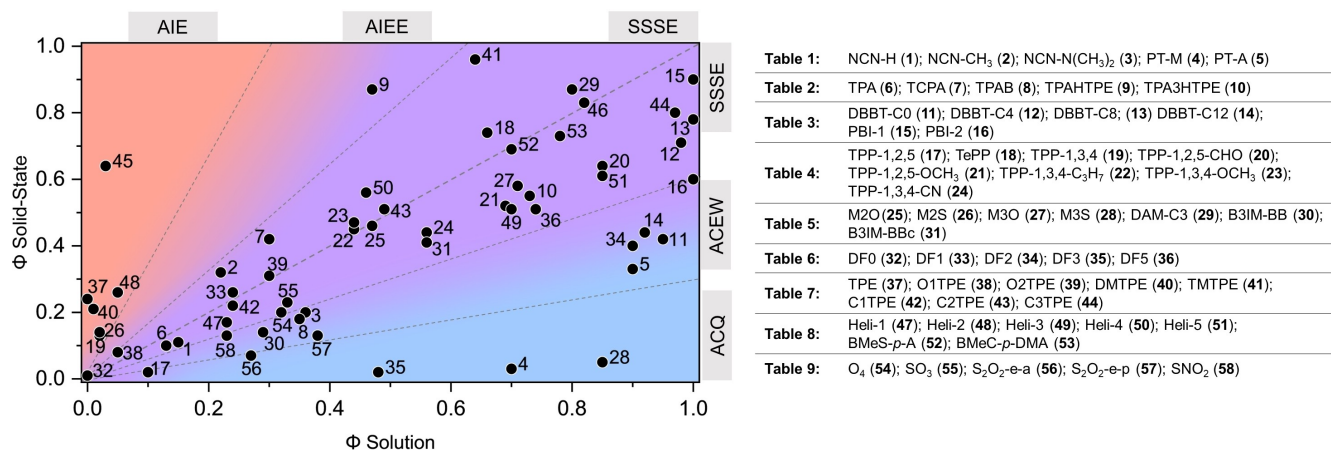


Figure 16. Benchmarking of all discussed examples in this minireview, sorted as they appear in the tables depicted (*vide supra*).

8. Conclusion and Outlook

The recognized importance of equally emissive behaviour in both solution and the solid-state has inspired many groups to investigate not only explanations for this contradictory phenomenon but also models, developments, and various applications. Therefore, this minireview aims to present the hitherto elaborated concepts based on their distinct approaches. In this regard, an attempt was made to shine light on SSSEs from a different angle by simplifying their molecular design into the two subgroups of classic and non-classic examples. Based on the acquired requirements for luminescence appearance, molecular subgroups known for either one of the two supposedly opposed observations of AIE and ACQ can be combined by spatial separation (classic SSSEs) or fused indistinguishably (non-classic SSSEs). The main criteria to achieve SSSE classification are invariable: sufficient conjugation and planarization together with rigidifying but not unlimitedly flexible motifs must be implemented into the luminophore design to suppress vibrational and rotational relaxation as well as stacking quenching effects in solution and the solid-state.

Thus far, it has been difficult to predict the results and explain solid-state emission properties because of various influencing factors like the packing structures and the arrangements of the individual emitters. This challenge also complicates the application and technological utilization of SSSEs, such as in optoelectronics and bioimaging. Therefore, further explorations of this nascent topic are expected to deepen the knowledge and extend the conceptual spectrum. For this, additional design and synthesis of novel emitters and the unification of researchers of different research fields are anticipated to help surpass the current challenges. Thus, this minireview provides an overview of established approaches and reported discoveries with the intended purpose to inspire the development of novel concepts.

Acknowledgements

JV and JD acknowledge the DFG - Deutsche Forschungsgemeinschaft for funding (Grant: VO 2383/1-1, project number: 405679982). Additionally, we wish to thank CENIDE and the ZMB for their support. Open Access funding enabled and organized by Projekt DEAL.

Conflict of Interest

The authors declare no conflict of interest.

Data Availability Statement

The data that support the findings of this study are available from the corresponding author upon reasonable request.

Keywords: aggregation · dual-state emission (DSE) · fluorescence · solution and solid-state emission (SSSE)

- [1] B. Valeur, M. N. Berberan-Santos, *Molecular Fluorescence: Principles and Applications*, Wiley-VCH; Wiley-VCH Verlag GmbH & Co. KGaA, Weinheim, Germany [Chichester, England], 2012.
- [2] J. R. Lakowicz, *Principles of Fluorescence Spectroscopy*, Springer, New York, 2006.
- [3] M. Y. Berezin, S. Achilefu, *Chem. Rev.* **2010**, *110*, 2641–2684.
- [4] G. Chen, W. Li, T. Zhou, Q. Peng, D. Zhai, H. Li, W. Z. Yuan, Y. Zhang, B. Z. Tang, *Adv. Mater.* **2015**, *27*, 4496–4501.
- [5] L. A. Rodríguez-Cortés, A. Navarro-Huerta, B. Rodríguez-Molina, *Matter* **2021**, *4*, 2622–2624.
- [6] N. A. Kukhta, M. R. Bryce, *Mater. Horiz.* **2021**, *8*, 33–55.
- [7] S. T. N. Sailaja, I. Maisuls, J. Kösters, A. Hepp, A. Faust, J. Voskuhl, C. A. Strassert, *Beilstein J. Org. Chem.* **2020**, *16*, 2960–2970.
- [8] S. Riebe, S. Adam, B. Roy, I. Maisuls, C. G. Daniliuc, J. Dubbert, C. A. Strassert, I. Schapiro, J. Voskuhl, *Chem. Asian J.* **2021**, *16*, 2307–2313.
- [9] J. L. Belmonte-Vázquez, Y. A. Amador-Sánchez, L. A. Rodríguez-Cortés, B. Rodríguez-Molina, *Chem. Mater.* **2021**, *33*, 7160–7184.
- [10] E. R. Jimenez, H. Rodríguez, *J. Mater. Sci.* **2020**, *55*, 1366–1387.
- [11] J. Mei, Y. Hong, J. W. Y. Lam, A. Qin, Y. Tang, B. Z. Tang, *Adv. Mater.* **2014**, *26*, 5429–5479.

- [12] J. B. Birks, *Photophysics of Aromatic Molecules*, Wiley-Interscience, London, New York, 1970.
- [13] F. Würthner, *Angew. Chem. Int. Ed.* **2020**, *59*, 14192–14196; *Angew. Chem.* **2020**, *59*, 14192–14196.
- [14] G. C. Schmidt, *Ann. Phys.* **1921**, *370*, 247–256.
- [15] G. Scheibe, *Angew. Chem.* **1936**, *49*, 658–658.
- [16] E. E. Jelley, *Nature* **1936**, *138*, 1009–1010.
- [17] F. Würthner, T. E. Kaiser, C. R. Saha-Möller, *Angew. Chem. Int. Ed.* **2011**, *50*, 3376–3410; *Angew. Chem.* **2011**, *123*, 3436–3473.
- [18] J. Luo, Z. Xie, J. W. Y. Lam, L. Cheng, B. Z. Tang, H. Chen, C. Qiu, H. S. Kwok, X. Zhan, Y. Liu, D. Zhu, *Chem. Commun.* **2001**, 1740–1741.
- [19] J. Mei, N. L. C. Leung, R. T. K. Kwok, J. W. Y. Lam, B. Z. Tang, *Chem. Rev.* **2015**, *115*, 11718–11940.
- [20] J. Yang, Z. Chi, W. Zhu, B. Z. Tang, Z. Li, *Sci. China Chem.* **2019**, *62*, 1090–1098.
- [21] N. L. C. Leung, N. Xie, W. Yuan, Y. Liu, Q. Wu, Q. Peng, Q. Miao, J. W. Y. Lam, B. Z. Tang, *Chem. Eur. J.* **2014**, *20*, 15349–15353.
- [22] N. J. Hestand, F. C. Spano, *Chem. Rev.* **2018**, *118*, 7069–7163.
- [23] M. Hayduk, T. Schaller, F. C. Niemeyer, K. Rudolph, G. H. Clever, F. Rizzo, J. Voskuhl, *Chem. Eur. J.* **2022**, 10.1002/chem.202201081.
- [24] G. Liang, J. W. Y. Lam, W. Qin, J. Li, N. Xie, B. Z. Tang, *Chem. Commun.* **2014**, *50*, 1725–1727.
- [25] S. Li, S. M. Langenegger, R. Häner, *Chem. Commun.* **2013**, *49*, 5835.
- [26] J. Gierschner, J. Shi, B. Milián-Medina, D. Roca-Sanjuán, S. Varghese, S. Park, *Adv. Opt. Mater.* **2021**, *9*, 2002251.
- [27] M. Schäferling, *Angew. Chem. Int. Ed.* **2012**, *51*, 3532–3554; *Angew. Chem.* **2012**, *124*, 3590–3614.
- [28] Q. Zhang, B. Li, S. Huang, H. Nomura, H. Tanaka, C. Adachi, *Nat. Photonics* **2014**, *8*, 326–332.
- [29] C. W. T. Leung, Y. Hong, S. Chen, E. Zhao, J. W. Y. Lam, B. Z. Tang, *J. Am. Chem. Soc.* **2013**, *135*, 62–65.
- [30] M. Jiang, X. Gu, J. W. Y. Lam, Y. Zhang, R. T. K. Kwok, K. S. Wong, B. Z. Tang, *Chem. Sci.* **2017**, *8*, 5440–5446.
- [31] J. Liang, B. Z. Tang, B. Liu, *Chem. Soc. Rev.* **2015**, *44*, 2798–2811.
- [32] A. Zimmermann, Q. Z. Jaber, J. Koch, S. Riebe, C. Vallet, K. Loza, M. Hayduk, K. B. Steinbuch, S. K. Knauer, M. Fridman, J. Voskuhl, *ChemBioChem* **2021**, *22*, 1563–1567.
- [33] L. Porrès, A. Holland, L.-O. Pålsson, A. P. Monkman, C. Kemp, A. Beeby, *J. Fluoresc.* **2006**, *16*, 267–273.
- [34] A. S. Klymchenko, *Acc. Chem. Res.* **2017**, *50*, 366–375.
- [35] D. Liese, G. Haberhauer, *Isr. J. Chem.* **2018**, *58*, 813–826.
- [36] R. Misra, S. P. Bhattacharyya, *Intramolecular Charge Transfer: Theory and Applications*, John Wiley & Sons, Wiley-VCH, Weinheim, **2018**.
- [37] V. S. Padalkar, S. Seki, *Chem. Soc. Rev.* **2016**, *45*, 169–202.
- [38] J. Chen, C. C. W. Law, J. W. Y. Lam, Y. Dong, S. M. F. Lo, I. D. Williams, D. Zhu, B. Z. Tang, *Chem. Mater.* **2003**, *15*, 1535–1546.
- [39] M. Rivera, L. Stojanović, R. Crespo-Otero, *J. Phys. Chem. A* **2021**, *125*, 1012–1024.
- [40] R. Crespo-Otero, Q. Li, L. Blancafort, *Chem. Asian J.* **2019**, *14*, 700–714.
- [41] S. Kumar, P. Singh, P. Kumar, R. Srivastava, S. K. Pal, S. Ghosh, *J. Phys. Chem. C* **2016**, *120*, 12723–12733.
- [42] M. Huang, R. Yu, K. Xu, S. Ye, S. Kuang, X. Zhu, Y. Wan, *Chem. Sci.* **2016**, *7*, 4485–4491.
- [43] Q. Zhao, X. A. Zhang, Q. Wei, J. Wang, X. Y. Shen, A. Qin, J. Z. Sun, B. Z. Tang, *Chem. Commun.* **2012**, *48*, 11671.
- [44] Q. Zeng, Z. Li, Y. Dong, C. Di, A. Qin, Y. Hong, L. Ji, Z. Zhu, C. K. W. Jim, G. Yu, Q. Li, Z. Li, Y. Liu, J. Qin, B. Z. Tang, *Chem. Commun.* **2007**, 70–72.
- [45] L. Zou, S. Guo, H. Lv, F. Chen, L. Wei, Y. Gong, Y. Liu, C. Wei, *Dyes Pigm.* **2022**, *198*, 109958.
- [46] P. Blanchard, C. Malacrida, C. Cabanetos, J. Roncali, S. Ludwigs, *Polym. Int.* **2019**, *68*, 589–606.
- [47] W. Dai, P. Liu, S. Guo, Z. Liu, M. Wang, J. Shi, B. Tong, T. Liu, Z. Cai, Y. Dong, *ACS Appl. Bio Mater.* **2019**, *2*, 3686–3692.
- [48] A. Patra, S. P. Anthony, T. P. Radhakrishnan, *Adv. Funct. Mater.* **2007**, *17*, 2077–2084.
- [49] J. Yin, Y. Ma, G. Li, M. Peng, W. Lin, *Coord. Chem. Rev.* **2020**, *412*, 213257.
- [50] Y. Xu, L. Ren, D. Dang, Y. Zhi, X. Wang, L. Meng, *Chem. Eur. J.* **2018**, *24*, 10383–10389.
- [51] B. Zhang, H. Soleimaninejad, D. J. Jones, J. M. White, K. P. Ghiggino, T. A. Smith, W. W. H. Wong, *Chem. Mater.* **2017**, *29*, 8395–8403.
- [52] T. Weil, T. Vosch, J. Hofkens, K. Peneva, K. Müllen, *Angew. Chem. Int. Ed.* **2010**, *49*, 9068–9093; *Angew. Chem.* **2010**, *122*, 9252–9278.
- [53] D. Schmidt, M. Stolte, J. Süß, A. Liess, V. Stepanenko, F. Würthner, *Angew. Chem. Int. Ed.* **2019**, *58*, 13385–13389; *Angew. Chem.* **2019**, *131*, 13519–13523.
- [54] M. Stolte, T. Schembri, J. Süß, D. Schmidt, A.-M. Krause, M. O. Vysotsky, F. Würthner, *Chem. Mater.* **2020**, *32*, 6222–6236.
- [55] Y. Lei, Q. Liu, L. Dong, Z. Cai, J. Shi, J. Zhi, B. Tong, Y. Dong, *Chem. Eur. J.* **2018**, *24*, 14269–14274.
- [56] Y. Li, Y. Lei, L. Dong, L. Zhang, J. Zhi, J. Shi, B. Tong, Y. Dong, *Chem. Eur. J.* **2019**, *25*, 573–581.
- [57] Y. Lei, W. Dai, Z. Liu, S. Guo, Z. Cai, J. Shi, X. Zheng, J. Zhi, B. Tong, Y. Dong, *Mater. Chem. Front.* **2019**, *3*, 284–291.
- [58] J. Wang, Z. Liu, S. Yang, Y. Lin, Z. Lin, Q. Ling, *Chem. Eur. J.* **2018**, *24*, 322–326.
- [59] J. Price, E. Albright, A. Decken, S. Eisler, *Org. Biomol. Chem.* **2019**, *17*, 9562–9566.
- [60] X. Zheng, J. Wang, D. Xiao, H. Chen, Z. Lin, Q. Ling, *Dyes Pigm.* **2021**, *187*, 109113.
- [61] A. C. Sedgwick, L. Wu, H.-H. Han, S. D. Bull, X.-P. He, T. D. James, J. L. Sessler, B. Z. Tang, H. Tian, J. Yoon, *Chem. Soc. Rev.* **2018**, *47*, 8842–8880.
- [62] T. Stoerkler, T. Parlat, A. D. Laurent, D. Jacquemin, G. Ulrich, J. Massue, *Molecules* **2022**, *27*, 2443.
- [63] D. D. La, S. V. Bhosale, L. A. Jones, S. V. Bhosale, *ACS Appl. Mater. Interfaces* **2018**, *10*, 12189–12216.
- [64] H.-T. Feng, Y.-X. Yuan, J.-B. Xiong, Y.-S. Zheng, B. Z. Tang, *Chem. Soc. Rev.* **2018**, *47*, 7452–7476.
- [65] J. Shi, N. Chang, C. Li, J. Mei, C. Deng, X. Luo, Z. Liu, Z. Bo, Y. Q. Dong, B. Z. Tang, *Chem. Commun.* **2012**, *48*, 10675–10677.
- [66] G.-F. Zhang, Z.-Q. Chen, M. P. Aldred, Z. Hu, T. Chen, Z. Huang, X. Meng, M.-Q. Zhu, *Chem. Commun.* **2014**, *50*, 12058–12060.
- [67] J.-B. Xiong, H.-T. Feng, J.-P. Sun, W.-Z. Xie, D. Yang, M. Liu, Y.-S. Zheng, *J. Am. Chem. Soc.* **2016**, *138*, 11469–11472.
- [68] X. Zheng, W. Zhu, C. Zhang, Y. Zhang, C. Zhong, H. Li, G. Xie, X. Wang, C. Yang, *J. Am. Chem. Soc.* **2019**, *141*, 4704–4710.
- [69] H. Oyama, K. Nakano, T. Harada, R. Kuroda, M. Naito, K. Nobusawa, K. Nozaki, *Org. Lett.* **2013**, *15*, 2104–2107.
- [70] M. Li, Y. Niu, X. Zhu, Q. Peng, H.-Y. Lu, A. Xia, C.-F. Chen, *Chem. Commun.* **2014**, *50*, 2993–2995.
- [71] J. R. Reimers, *J. Chem. Phys.* **2001**, *115*, 9103–9109.
- [72] Y. Shen, C.-F. Chen, *Chem. Rev.* **2012**, *112*, 1463–1535.
- [73] M. Li, W. Yao, J.-D. Chen, H.-Y. Lu, Y. Zhao, C.-F. Chen, *J. Mater. Chem. C* **2014**, *2*, 8373–8380.
- [74] T. Beppu, K. Tomiguchi, A. Masuhara, Y.-J. Pu, H. Katagiri, *Angew. Chem. Int. Ed.* **2015**, *54*, 7332–7335; *Angew. Chem.* **2015**, *127*, 7440–7443.
- [75] R. Huang, B. Liu, C. Wang, Y. Wang, H. Zhang, *J. Phys. Chem. C* **2018**, *122*, 10510–10518.
- [76] M. D. Watson, A. Fechtenkötter, K. Müllen, *Chem. Rev.* **2001**, *101*, 1267–1300.
- [77] J. Shaya, F. Fontaine-Vive, B. Y. Michel, A. Burger, *Chem. Eur. J.* **2016**, *22*, 10627–10637.
- [78] T. Beppu, S. Kawata, N. Aizawa, Y.-J. Pu, Y. Abe, Y. Ohba, H. Katagiri, *ChemPlusChem* **2014**, *79*, 536–545.
- [79] S. Kang, Y. Jung, J. Jung, K.-H. Park, D. Kim, *Dyes Pigm.* **2021**, *185*, 108939.
- [80] Y. Jung, J. H. Jin, Y. Kim, J. H. Oh, H. Moon, H. Jeong, J. Kim, Y. K. Park, Y. Oh, S. Park, D. Kim, *Org. Biomol. Chem.* **2022**, *20*, 5423–5433.
- [81] J. Kim, J. H. Oh, D. Kim, *Org. Biomol. Chem.* **2021**, *19*, 933–946.
- [82] W. Xi, J. Yu, M. Wei, Q. Qiu, P. Xu, Z. Qian, H. Feng, *Chem. Eur. J.* **2020**, *26*, 3733–3737.
- [83] L. K. Hiscock, C. Yao, W. G. Skene, L. N. Dawe, K. E. Maly, *J. Org. Chem.* **2019**, *84*, 15530–15537.

Manuscript received: August 9, 2022
Accepted manuscript online: October 4, 2022
Version of record online: November 14, 2022